# PREPARATION AND CHARACTERIZATION OF POROUS CHITOSAN-ORGANICALLY MODIFIED MONTMORILLONITE-HYDROXYAPATITE (CS-OM-HA) COMPOSITES FOR BIOMEDICAL APPLICATIONS

A THESIS SUBMITTED IN PARTIAL FULFILLMENT

OF THE REQUIREMENT FOR THE DEGREE OF

**Master of Technology**

**in**

**Biotechnology**

**by**


**Sumanta Kar**

**213BM2026**


**Under the supervision of**


**Dr. A. Thirugnanam**

**Department of Biotechnology and Medical Engineering**

**National Institute of Technology Rourkela**

**Rourkela, Odisha, 769008, India**


**30th May 2015**


**Department of Biotechnology and Medical Engineering**

**National Institute of Technology Rourkela**

**Rourkela 769008, Odisha (India)**

## *Certificate*

This is to certify that the thesis entitled "**Preparation and characterization of porous chitosan -organically modified montmorillonite-hydroxyapatite (CS-OM-HA) composites for biomedical applications**" by **Sumanta Kar (213BM2026),** in partial fulfillment of the requirements for the award of the degree of Master of Technology in Biotechnology during session 2013-2015 in the Department of Biotechnology and Medical Engineering, National Institute of Technology Rourkela, is an authentic work carried out by him under my supervision. To the best of my knowledge, the matter embodied in the thesis has not been submitted to any other University/Institute for the award of any degree or diploma.

**Place: NIT Rourkela**

**Date: 30th May, 2015**

**Dr. A. Thirugnanam (Supervisor)**

**Assistant Professor**

**Biotechnology and Medical Engineering**

**National Institute of Technology**

**Rourkela-769 008, Odisha (India)**

# Acknowledgement

Successful completion of this project is the outcome of consistent guidance and assistance from many people, faculty and friends and I am extremely fortunate to have got these all along the completion of the project.

I owe my profound gratitude and respect to my project guide, **Prof. A. Thirugnanam**, Department of Biotechnology and Medical Engineering, NIT Rourkela for his invaluable academic support and professional guidance, regular encouragement and motivation at various stages of this project.

I place on record my sincere gratitude to **Prof. Krishna Pramanik**, Head of Department, Department of Biotechnology and Medical Engineering, NIT Rourkela for her constant encouragement.

I would like to thank **Ms. Tejinder Kaur, Mr. Omkar Majumder,** and **Mr. Basil Mathai,** Department of Biotechnology and Medical Engineering, NIT Rourkela, for their regular support, help and motivation.

I would also thank my Institution and my faculty members without whom this project would have been a distant reality. I also extend my thanks to my family, friends, and well-wishers.

**Place: NIT Rourkela**

**Date: 30th May, 2015**

**Sumanta Kar**

**212BM2026**

**Biotechnology and Medical Engineering**

**National Institute of Technology**

**Rourkela-769008, Odisha (India)**

# CONTENTS

# LIST OF FIGURES

# LIST OF TABLES

# ABSTRACT

In this study, a porous chitosan (CS)-organically modified montmorillonite (OM)-hydroxyapatite (HA) composite was developed by combining microwave irradiation and gas foaming method. The prepared composite was characterized using X-ray diffraction (XRD), attenuated total reflectance-fourier transform infrared (ATR-FTIR) spectroscopy, and scanning electron microscopy (SEM). The synergistic effect of OM and HA on the mechanical and *in vitro* biological properties (swelling, degradation and protein adsorption) of the composite were evaluated. In addition, the *in vitro* bioactivity of the composites was studied in simulated body fluid (SBF) for 21 days. The XRD results revealed the formation of an exfoliated structure upon incorporation of OM. ATR-FTIR studies indicated strong molecular interaction among the three different components of the composite. The CS-OM-HA composites exhibited a reduction in swelling, degradation and protein adsorption; whereas an enhancement in bioactivity was witnessed as evidenced by SEM analysis. Furthermore, the CS-OM-HA composites showed a significant enhancement in mechanical (tensile) property in comparison with pure chitosan (CS) and CS-OM composites. An *in vitro* cytotoxic assay was also performed to determine the biocompatibility of the prepared CS based composites. The results showed that the prepared CS based composites were non-toxic. From the study, it can be concluded that the novel CS-OM-HA composite with improved *in vitro* biological and mechanical properties has wide potential in non-load bearing orthopedic applications.



***Keywords:*** **Chitosan, hydroxyapatite, organically modified montmorillonite, bioactivity, biocompatibility**

# CHAPTER 1

# INTRODUCTION

# 1. INTRODUCTION

The use of porous polymer/bioceramic composites to repair and replace injured bone tissue has been a well-established area of interest. The fabrication of materials that can match both mechanical and biological properties of human bone tissue matrix is a critical concern in orthopedic treatment. Keeping this aforementioned fact in mind, attempts have been made to recreate nanoscale topographical cues from the extracellular environment with improved levels of biofunctionality [1].

Chitosan (CS) consists of D-glucosamine and N-acetyl glucosamine units linked by β (1-4)-glycosidic bonds, deacetylated form of the natural polymer chitin. Chitosan is widely used in making bone grafts because of its structural similarity to the various glycosaminoglycans (GAGs) found in the extracellular matrix (ECM) of bone, osteoconductivity to enhance bone formation both *in vitro* and *in vivo*, biocompatibility, non-toxic degradation products etc. [2]. Chitosan forms polyelectrolyte complexes (PECs) due to its polycationic nature [3]. Unlike chitosan's biocompatibility, its thermal stability, hardness and bioactivity need to be improved by incorporation of biologically active molecules like hydroxyapatite [4]. Glutaraldehyde (GA) ($CH_2(CH_2CHO)_2$), is used as a cross-linking agent in the preparation of chitosan based bone grafts ,despite of its cytotoxicity [5].

Hydroxyapatite (HA) [$Ca_{10}(PO_4)_6(OH)_2$], owing to its excellent bioactivity, osteoconductivity, and chemical and physical resemblance to the mineral constituents of human bone, has been a preferred bioceramic in the fabrication of composite for orthopedic applications. Hydroxyapatite promotes the interaction between host bone and grafted material by binding to the natural bone through biochemical bonding [6]. However, HA based scaffolds are extremely brittle. They do not have enough mechanical integrity to be used as hard-tissue implants. In order to improve mechanical properties of hydroxyapatite scaffold, most often chitosan is incorporated in hydroxyapatite while preparing composites. The formation of coordination bonds between the amine groups of chitosan and calcium ions of HA leads to the enhancement of mechanical properties [7]. Kong *et al.* have synthesized porous chitosan/HA composite scaffolds using the lyophilisation method with improved biocompatibility and bioactivity as compared to pure chitosan scaffolds. Addition of HA

resulted in more apatite formation on the composite scaffolds than that on the pure chitosan scaffolds. Incorporation of HA also increased the mechanical property composite scaffolds [8-10]. The results of other studies have shown that chitosan/HA composite scaffolds were found to be osteoconductive in nature [11].

Montmorillonite (MMT) is basically nanoclay that acts as a filler material due to its high surface area to volume ratio [12]. Studies have reported that incorporation of MMT even in lower concentration can greatly enhance the mechanical properties of the composites [13]. MMT clay can be modified organically by exchanging the cations present in the interlayer with cationic surfactants such as alkylammonium salts to increase its interlayer d-spacing so as to facilitate the exfoliation of the silicate layers within the polymer matrix. In this work, montmorillonite has been modified organically with alkylammonium salts in order to improve its miscibility with the polymer matrix [15].

Microwave chemistry has been receiving remarkable attention, owing to its powerful thermal effect that helps in completion of the reactions in the shortest possible time by means of rapid and uniform heating [16]. Beşkardeş *et al.* have reported synthesis of chitosan–hydroxyapatite superporous hydrogel composites using a combination of microwave irradiation and gas foaming with improved porosity and osteocompatibility [17].

There have been a few studies focused on the use of MMT clay and MMT-HA along with CS for preparing nanocomposite for orthopedic applications [12-15, 18-21]. Ambre *et al.* developed a novel nanocomposite containing chitosan/polygalacturonic acid-hydroxyapatite-5-aminovaleric acid modified montmorillonite (MMT) clay using freeze drying technique, with improved mechanical, osteoconductivity for bone tissue engineering [14]. But the use of MMT clays modified with alkylammonium salts in the preparation of polymer composites for non-load bearing for orthopedic applications is not reported in literature. This work aims at developing a novel chitosan (CS)-organically modified montmorillonite (OM)-hydroxyapatite (HA) porous composites with improved physicochemical, *in vitro* biological and mechanical properties for non-load bearing orthopedic applications by combining microwave irradiation and gas foaming method. Sodium carbonate was used as gas blower in the experiment that resulted in release of $CO_2$ and a porous composite was formed. Synthesized composites were

carefully studied using X-ray diffraction (XRD), attenuated total reflectance-fourier transform infrared spectroscopy (ATR-FTIR), and scanning electron microscopy (SEM). Furthermore, mechanical properties and *in vitro* biological studies such as, swelling, degradation, bioactivity, protein adsorption and cytotoxicity were carried out to establish its relevance as a biomaterial for non-load bearing orthopedic applications.

# CHAPTER 2

# LITERATURE REVIEW

# 2. LITERATURE REVIEW

In recent years, there has been a significant progress in the fields of organ transplantation and surgical reconstruction to treat the loss of organs or bone tissue. However, the shortcomings associated with autografting and allografting transplantation, such as inherent donor site limitations, tissue rejection and disease transfer respectively, have paved the way of the development of making novel bone grafts. The composites made up of ceramic and polymeric materials ought to exhibit excellent degradation, biocompatibility and mechanical strength [22].

## 2.1 Biodegradability

Biodegradable polymers are supposed to decompose in a living body without leaving any of its degradation products in tissues. These polymers and their degradation products are not supposed to elicit any immunogenic reaction or any toxicity and their degradation rate should match with the curing rate of tissues. The polymers should have enough mechanical integrity to withstand the stress incurred on bone tissue during cycling loading and unloading [23].

## 2.2 Biocompatibility

Biocompatibility refers to the compatibility of a material with the host tissue that includes physical, chemical, biological and structural suitability of the material to the host tissue [24]. The tensile strength and toughness of bone are assigned the flexible collagen reinforced with HA [25].

## 2.3 Mechanical Strength

The mechanical strength of composites is of particular importance while making bone grafts, since they are closely linked to the structural stability and durability in practical applications. The composites ought to have enough mechanical strength to function properly form the time of implantation to the completion of tissue remodeling process. A reduction in composite porosity greatly enhances the mechanical properties. Studies have reported that increasing porosity have resulted in decrease of mechanical strength [20].

## 2.4 Polymer-Bioceramic composites

Chitosan has been choice of biopolymer candidates in making bone grafts because of non-toxic degradation products. Tang *et al.* fabricated chitosan/hydroxyapatite with excellent hard tissue biocompatibility and osteoconductivity [26]. Jayabalan *et al.* have reported a biocompatible and osteocompatible nanocomposite containing calcined HA nanoparticles [27]. The electrospun nanofibers of HA/chitosan with compositional and structural features close to the natural mineralized nanofibril counterparts were prepared by Zhang *et al.* for bone tissue engineering applications [28]. Kashiwazaki *et al.* investigated the biocompatibility and biodegradation of an innovative porous chitosan/hydroxyapatite nanocomposite synthesized using co-precipitation and porogen leaching [29]. Chitosan/poly vinyl alcohol electrospun nanofibers were prepared with an average diameter from 100 to 50 nm [30]. A macroporous bioactive chitosan/hydroxyapatite scaffold was synthesized through phase separation [31]. Zhao *et al.* fabricated a biodegradable 3D hydroxyapatite/chitosan–gelatin composite scaffold for bone tissue engineering applications [32]. In a similar study, Zhao *et al.* reported two types of composite scaffolds, chitosan–gelatin and hydroxyapatite/chitosan–gelatin. Hydroxyapatite/chitosan–gelatin composite scaffolds have shown better osteoinductivity [33]. Liuyun *et al.* prepared nanohydroxyapatite/chitosan/carboxymethyl cellulose biocompatible composite scaffolds by freeze-drying method. The results of *in vivo* showed that the scaffold has a good biocompatibility and can be used for bone tissue engineering [34].

## 2.5 Polymer-clay nanocomposites

The challenge of developing composites with adequate mechanical properties presents a unique problem in the field of tissue engineering. Polymer-clay nanocomposites (PCNs) seem to possess tremendous potential with regard to the aspect of achieving adequate mechanical properties. The use of MMT clay for the preparation of PCNs was pioneered by the Toyota research group in 1990 when they reported significant improvement in mechanical properties of the PCNs composed of low MMT clay loadings [35]. Recent studies have reported usage of modifiers to increase the miscibility of clay in the polymer. The backbone chain length and the functional groups present in the modifier affect the d-spacing of the clay. Also, it was found in this study that the backbone chain length of the modifier has similar

magnitude of influence on the d-spacing of the clay as that of the functional groups present in the modifier [36]. Montmorillonite's ability to absorb various toxins and cross the gastrointestinal barrier to facilitate drug delivery, encourage its use for tissue engineering applications [14]. Wang *et al.* developed a biopolymer chitosan/montmorillonite nanocomposite with improved thermal stability and mechanical properties [18]. Zhuang *et al.* prepared an intercalated gelatin/montmorillonite–chitosan nanocomposite with controlled *in vitro* degradation and excellent biocompatibility [19]. Zheng *et al*. synthesized a nanocomposite scaffold containing gelatin, montmorillonite and chitosan with improved mechanical properties and tailored degradation rate [13]. Katti *et al.* reported a novel chitosan/montmorillonite/hydroxyapatite nanocomposite with improved mechanical property and good biocompatibility for biomedical applications [21]. Ambre *et al.* fabricated a novel nanocomposite containing chitosan/polygalacturonic acid-hydroxyapatite-5-aminovaleric acid modified montmorillonite (MMT) clay using freeze drying technique, with improved mechanical, osteoconductivity for bone tissue engineering [14]. Olad *et al.* prepared a novel chitosan–gelatin/nanohydroxyapatite–montmorillonite composite scaffold using freeze drying, with improved physicochemical, *in vitro* biological and mechanical properties for tissue engineering applications [20].

## 2.6 Microwave irradiation and its incorporation in composite synthesis

Microwave has received an unprecedented attention owing to its powerful thermal effect that helps in completion of the reactions in the shortest possible time by means of rapid and uniform heating [16]. Ge *et al.* used microwave irradiation to synthesize and characterize a novel adsorbent containing chitosan cross-linked with both epichlorohydrin and EDTA dianhydride [37]. Lee *et al.* made the use of microwave heating to promote thermal crosslinking of polyethylene glycol containing microstructures. [38]. Shi *et al*. prepared a cross-linked poly (N-isopropyl-acryl amide) hydrogels in a microwave oven with porous morphology and equilibrium swelling ratios [39]. Beşkardeş *et al.* used combination of microwave irradiation and gas foaming to synthesize chitosan–hydroxyapatite superporous hydrogel composites with improved porosity and osteocompatibility [17].

## 2.7 Objective of the work

The objective of this work was to develop porous chitosan (CS)-organically modified montmorillonite (OM)-hydroxyapatite (HA) composites by combining microwave irradiation and gas foaming and to characterize it for mechanical, physiochemical, and *in vitro* biological properties.

# CHAPTER 3

# MATERIALS AND METHODS

# 3. MATERIALS AND METHODS

## 3.1 Materials

Chitosan (CS) (medium molecular weight, degree of deacetylation 75%), montmorillonite (MMT), diammonium phosphate ($(NH_4)_2HPO_4$), calcium nitrate tetrahydrate (Ca $(NO_3)_2.4H_2O$), cetyl trimethyl ammonium bromide (CTAB), bovine serum albumin (BSA), 3-(4,5-dimethylthiazol-2-yl)-2,5-diphenyltetrazolium bromide (MTT), penicillin-streptomycin solution obtained from Himedia, India were used in this study. Dulbecco modified eagle's medium (DMEM) was purchased from Gibco, India. Fetal Bovine Serum (FBS) was procured from Sigma Aldrich, India and dimethyl sulphoxide (DMSO) was supplied by SRL, India. All the chemical reagents were analytical grade and were used without further purification. Distilled water was used throughout the experiment.

## 3.2 Methods

### *3.2.1 Solid state synthesis of hydroxyapatite (HA) ($Ca_{10}(PO_4)_6(OH)_2$)*

To prepare HA via solid state route, diammonium Phosphate ($(NH_4)_2HPO_4$) and calcium nitrate tetrahydrate (Ca $(NO_3)_2.4H_2O$) were used as precursors of phosphate and calcium, respectively. Sodium bicarbonate ($NaHCO_3$) was used as a gas foaming agent. HA was prepared using the solid-state reaction at room temperature according to the following chemical equation [40]:

$$6((NH_4)_2HPO_4 + 10\ Ca\ (NO_3)_2.4H_2O + 8\ NaHCO_3 \longrightarrow Ca_{10}\ (PO_4)_6\ (OH)_2\downarrow + 12\ NH_4NO_3 + 8\ NaNO_3 + 8\ CO_2\uparrow + 10\ H_2O \quad (1)$$

The desired Ca/P ratio of 1.67 of HA was kept constant. The reactants were blended and grounded using mortar and pestle. After aging 24 h, the sample was washed several times with ethanol and de-ionized water to ensure complete removal of the by-product, followed by drying at 80ºC in an oven for 6 h. The dried sample was calcined at 650 $^0$C for 1 h to obtain HA (Fig. 1).

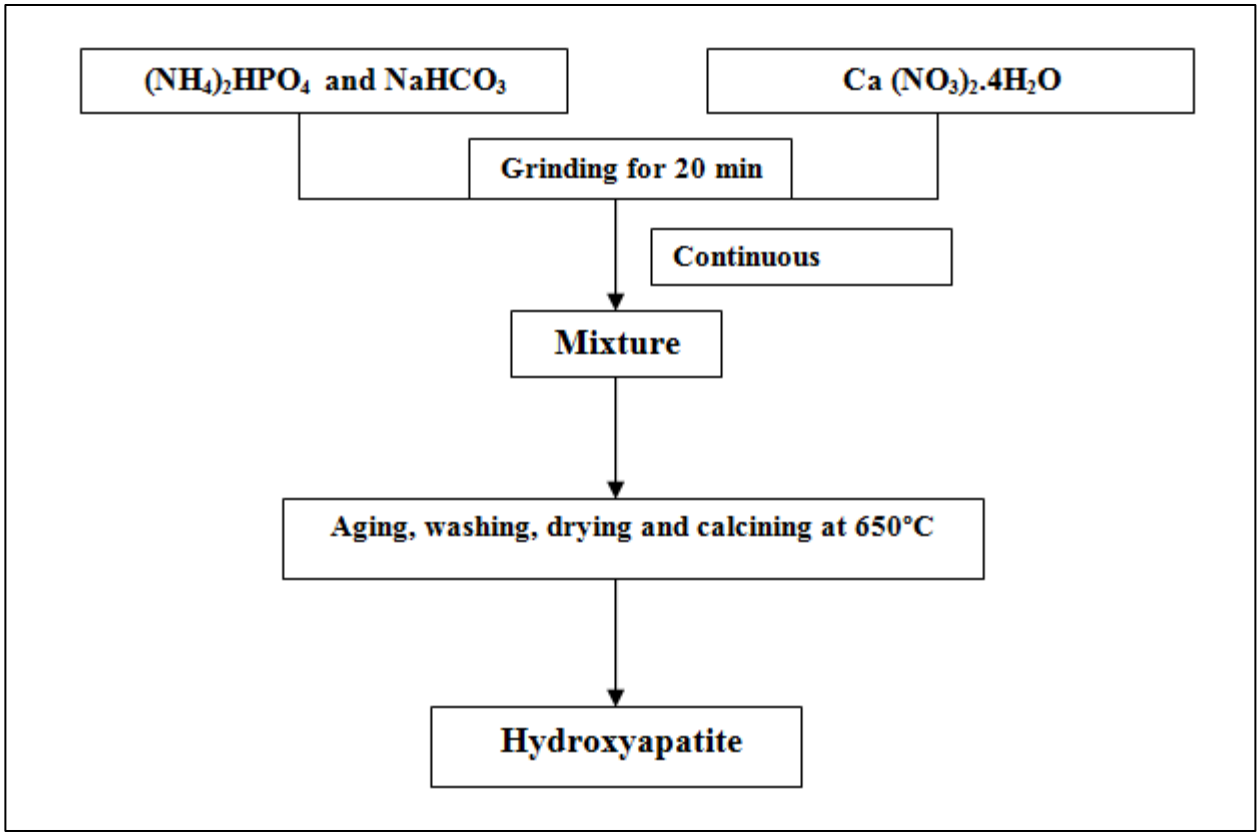


**Fig. 1 Flow chart of solid state synthesis of hydroxyapatite.**

### *3.2.2 Organic modification of montmorillonite (MMT)*

Initially, 10 g of MMT was added to a 1000 ml of distilled water and stirred it at 80 $^0$C for 24 h. Another solution containing Cetyl trimethyl ammonium bromide (CTAB) was prepared by adding 5 g of CTAB to 100 ml of distilled water. Freshly prepared CTAB solution was added to the MMT solution and stirred it for another 10 h to accomplish the cationic-exchange reaction. The final sample was filtered and dried to obtain organically modified montmorillonite (OM).

### *3.2.3 Preparation of porous chitosan-organically modified montmorillonite-hydroxyapatite (CS-OM-HA) composite*

Chitosan solution was prepared by dissolving 2 % (w/v) chitosan in 2 % (v/v) acetic acid solution with stirring at room temperature to get a perfectly transparent solution. Then

OM (10 wt%, respect to chitosan amount) was dispersed in the CS solution for 24 h by continuous stirring on a magnetic stirrer at 500 rpm and this suspension was further ultrasonicated for 5 min to get a homogeneous solution.

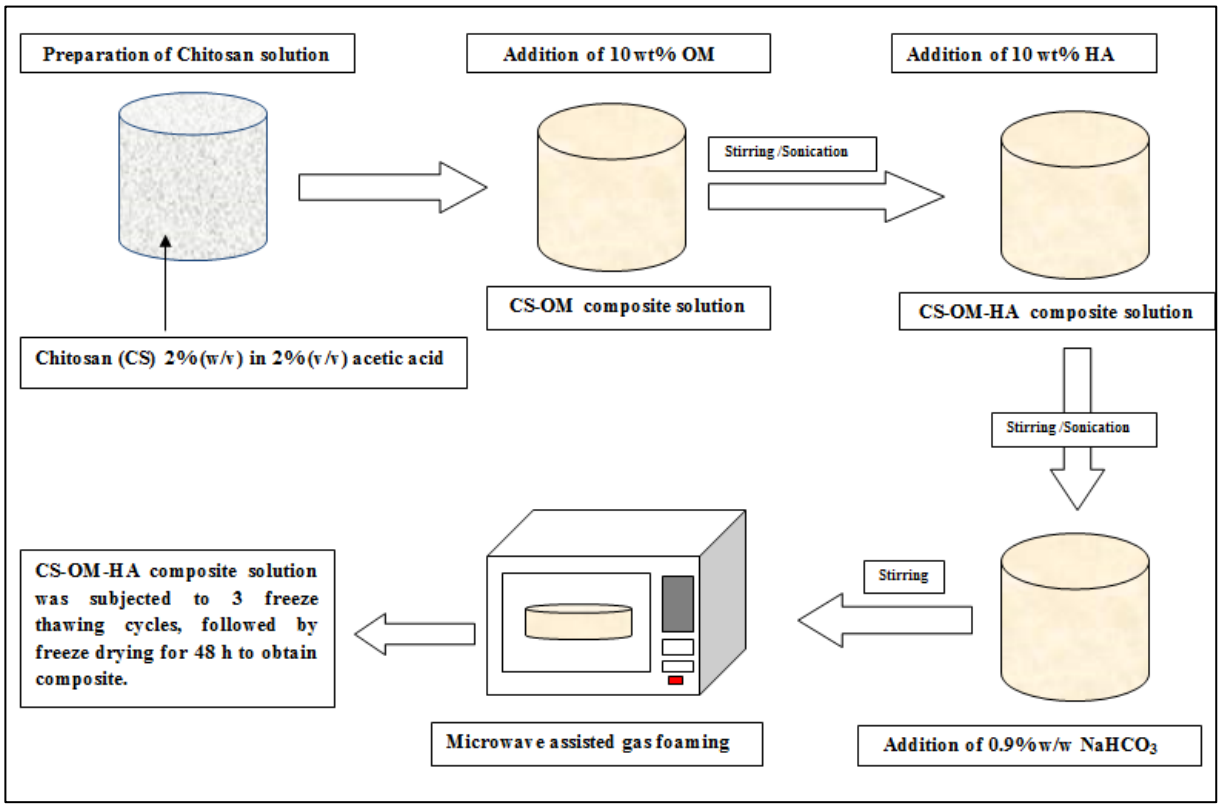


**Fig. 2 Schematic representation for the preparation of porous CS-OM-HA composite.**

In the second step, HA (10 wt%, respect to chitosan amount) was disseminated in the CS-OM solution for 24h by continuous stirring on a magnetic stirrer at 500 rpm. In order to get a perfect dispersion, solution was further ultrasonicated for 5 min and then glutaraldehyde solution (1%) was added drop wise and stirred for another 20 min at room temperature. Prior to pouring the cross-linked product into a 12-well polystyrene tissue culture plate, 0.9% (w/w) sodium bicarbonate was added to it. Finally, gas foaming took place in a kitchen microwave oven with 300W for 20s. The synthesized samples were then kept for freezing in refrigerator at -20ºC for 22 h and exposed at 37ºC for 2 h for thawing to complete one freeze thawing cycle. This cycle was repeated twice to obtain CS–OM–HA composites and then composites were subjected to freeze drying for 48 h in order to remove water content. Same procedure was used to synthesize pure CS and CS–OM composites to compare with CS–OM–HA

composite as schematically represented in Fig. 2.

## 3.3 Physicochemical Characterization

### *3.3.1 Scanning electron microscopy*

The surface morphology and pore size of the prepared composites (CS, CS-OM and CS-OM-HA) were examined under the scanning electron microscope (SEM) (JEOL JSM 6480LV, USA). Prior to analysis, the samples were cut into thin slices and coated with gold using a sputter coater.

### *3.3.2 X-ray diffraction analysis*

The XRD patterns of MMT, OM were obtained in the scan range of 2θ=3-40º whereas, the XRD patterns of HA was obtained at 2θ=20º-60º, respectively. The X-ray diffraction (XRD) patterns of composites (CS, CS-OM and CS-OM-HA) were obtained for a scan range of 2θ=3-60º to investigate the phase content of the composites. All the experiments were done at a scan rate of 5º/min with a step size of 0.05º, using Rigaku Ultima IV diffractometer (Japan) using CuKα radiation (λ=1.5418 Å).

### *3.3.3 Attenuated total reflectance-fourier transform infrared (ATR-FTIR) spectroscopy*

Attenuated total reflectance-fourier transform infrared (ATR-FTIR) spectra of individual components ( MMT, OM, HA) as well as the composite (CS, CS-OM, and CS-OM-HA) were obtained using Bruker, Alpha E spectrophotometer (Germany) in the range of 4000-520 $cm^{-1}$ at a spectral resolution of 4 $cm^{-1}$.

## 3.4 Mechanical (tensile) properties

The tensile properties of the composites were evaluated using a universal testing machine (UTM) (ElectroPuls E1000, Instron, UK). Tensile test was carried out at according to ASTM D3039 standard [42]. The testing was done at room temperature with a crosshead speed of 2 mm/min. A load cell of 250 N was used.

## 3.5 *In vitro* biological evaluation

### *3.5.1 Water absorption study (swelling test)*

The water absorption content of samples were determined by immersing the samples (with size of size 1cm x 1cm) in phosphate-buffered saline (PBS, pH=7.4) at room temperature for 24 h. The dry weights of the composites were calculated prior to immersion ($W_d$). Composites were immersed in PBS and their wet weights were recorded ($W_w$) after a predetermined time (24 h).The swelling percentage $S_w$ (%) was determined using the following equation [20]:

$$\boldsymbol{S_w(\%) = \frac{W_w - W_d}{W_w} X 100\%} \qquad (2)$$

where $W_w$ and $W_d$ represented the wet and dry weights of the composites, respectively. Three samples were tested for each system and the average values were taken.

### *3.5.2 In vitro degradation*

The *in vitro* degradation of the composites (of size 1 cm x 1 cm) was carried out by incubating the samples in PBS at 37°C. The initial weights of the composites were determined before immersing ($W_0$) into PBS. At regular intervals, the samples were taken out from the PBS, rinsed with distilled water and dried in hot air oven for 4 days prior to recording the weight ($W_t$). The degradation percentage *D (%)* was determined by the following equation [13]:

$$\mathbf{D\ (\%) = \frac{W_0 - W_t}{W_0}\ X\ 100\%} \qquad (3)$$

where $W_0$ and $W_t$ represented the initial and weights at time *t* (after 4 days), respectively. Three samples were tested for each system and the average values were taken.

### *3.5.3 In vitro bioactivity study*

The *in vitro* bioactivity of the composite was evaluated by examining the apatite formation on the samples after immersing in simulated body fluid (SBF). The SBF solution was prepared as per the protocol suggested by Kokubo *et al.* [41]. The samples were (of size 1x1 $cm^2$) incubated in simulated body fluid (SBF) at 37°C in a constant temperature water bath for 21 days. The samples were removed, rinsed with distilled water and dried at 37°C for 12 h. The samples were observed under scanning electron microscopy (SEM) to study the morphology of the apatite formed.

### *3.5.4 Protein adsorption study*

Composites (of size 1 cm x 1cm) were treated with PBS for 2 h prior to incubating in 1 ml of bovine serum albumin (BSA) solution (1 mg/ml BSA in PBS) at 37 °C for 24 h. After 24 h the samples were removed and centrifuged at 4000 rpm for 10 min. The amount of adsorbed protein was quantified using Bradford assay. Initially, 100 µl aliquot of the non-adsorbed protein solution was mixed with 1 ml of Bradford reagent and 2 ml of distilled water. The protein concentration was determined by UV spectrophotometer (double beam spectrometer 2203, SYSTRONICS, India) measurement at 595 nm. Measurements were performed in triplicates for each time.

### *3.4.5 Cell viability assay*

Cell culture studies were conducted using MG 63 cell line from NCCS, Pune, India. Dulbecco's modified eagle's media (DMEM) supplemented with 10% FBS and penicillin-streptomycin was used to culture osteoblast cells. Prior to cell seeding, the composites were placed in a 24-well culture plates and incubated with culture medium for 3 h at 37ºC in a humidified incubator with 5% $CO_2$. Then cells were seeded drop wise on the composites ($1x10^4$ cells/100 µl of medium/composite) after removing culture medium from the composite. Subsequently, the cell seeded composites were kept at 37ºC in a humidified incubator with 5% $CO_2$ for 48 h in order to allow the cells to attach to the composites. The cell viability on the composite constructs was measured using 3-(4, 5-dimethylthiazol-2-yl)-2, 5-diphenyltetrazolium bromide (MTT) assay. The samples were washed twice with PBS and

incubated with fresh culture medium containing 20 µl MTT solution (5 mg/ ml) at 37ºC for 4 h in a humidified incubator of 5% $CO_2$. The MTT solution was removed and 1 ml of dimethyl sulphoxide (DMSO) was added into each well in order to dissolve the formazan crystals. The absorbance of this solution was quantified by UV spectrophotometer (double beam spectrometer 2203, SYSTRONICS, India) at 570 nm. Experiments were performed in triplicates.

# CHAPTER 4

# RESULTS AND DISCUSSION

# 4. RESULTS AND DISCUSSION

## 4.1 Scanning electron microscopy

The composites with an adequate pore size and pore size distribution for ingrowths of cells and diffusion of nutrients should be used in orthopedic engineering. SEM micrographs of CS based composites are shown in Fig. 3. All the composites were appeared to be porous and have pore size above 100 μm.

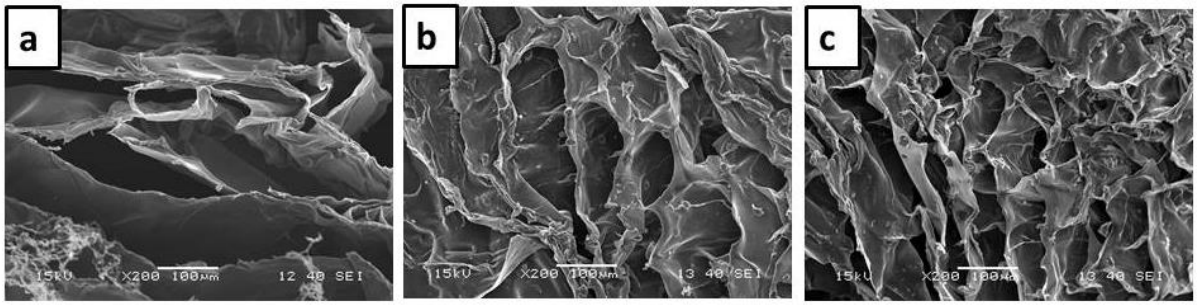


**Fig. 3 SEM micrographs of (a) CS, (b) CS-OM, and (c) CS-OM-HA composites.**

It is quite evident from the microstructures that the inclusion of OM and HA had reduced the pore sizes of composites (CS-OM, CS-OM-HA) as compared to pure CS. SEM micrographs also revealed the uniform distribution of both HA and OM particles in the chitosan matrix as there were no evidence of agglomeration. The carboxyl (-COOH) and amine ($-NH_2$) groups of chitosan may have interacted with $Ca^{+2}$ and $PO_4^{-3}$ groups of HA, respectively. The hydrophilicity and polycationic nature of chitosan facilitate the dispersion of silicate layers in the polymer matrix. These interactions may have played a pivotal role in the uniform distribution of both HA and OM. Yang *et al.* have reported that the pore size of scaffolds should be in the range of 65–300 μm for osteoblast proliferation and growth [43]. The pore size of the composites obtained from this study is within the reported range thus favoring the cell growth and proliferation of osteocytes.

## 4.2 X-ray diffraction analysis

The XRD patterns were obtained to check the presence of impurities and structural

phases in the composites. The XRD patterns of the individual components (MMT, OM, HA) as well as the chitosan (CS) composites are shown in the Fig.4. The XRD patterns of pristine MMT correspond to JCPDS no. 13-0259 (Fig. 4 a). The peak position for pristine MMT is found at 2θ=6.9º but surface modification by surfactant CTAB has resulted into a peak shift in XRD pattern of OM (2θ=4.7º). The decrease in 2θ relates to increase in interlayer d-spacing of OM due to organic modification [15]. The XRD patterns of the HA synthesized through solid state route corresponds to JCPDS no. 72-1243, confirming formation of HA phase (Fig. 4(b)).Strongest diffraction peaks of HA were found at 2θ values of 25.9º (002), 31.7º (211), 32.1º (112) and 32.9º (300). The crystallite size of the synthesized powders was calculated using Scherrer's formula and was found to be 65 nm. The fraction of crystalline phase ($X_c$) in HA powder has been calculated by the following equation [44]:

$$X_c = 1 - \frac{V_{112/300}}{I_{300}} \quad (4)$$

Where, $I_{300}$ is the intensity of the (300) diffraction peak and $V_{112/300}$ the intensity of the hollow between (112) and (300) diffraction peaks. The estimated crystallinity degree of HA was found to be about 38%.

Pendekal *et al.* have reported that chitosan powder has two characteristics peaks (2θ=20.02º, 10.53º) [45]. In Fig 4 b pure CS showed a broad amorphous peak at 2θ=22.8º which was found to be slightly shifted from the standard diffraction peak at 2θ=20.02º. This may be due to the interaction between acetic acid and chitosan that hinders the formation of inter-and intramolecular hydrogen bonds in CS, leading to a less packed conformation [20]. The characteristics peak of OM at 2θ=4.7º was not observed in the XRD patterns of CS-OM and CS-OM-HA composite scaffolds, confirming the formation of an exfoliated structure [45]. The XRD pattern of CS-OM-HA composite showed the diffraction peaks at 26º and 31.7º, indicating presence of HA in the composite. Furthermore, the peaks at 22.8º and 26.5º in both CS-OM and CS-OM-HA composite scaffolds were attributed to the presence of CS and OM, respectively.

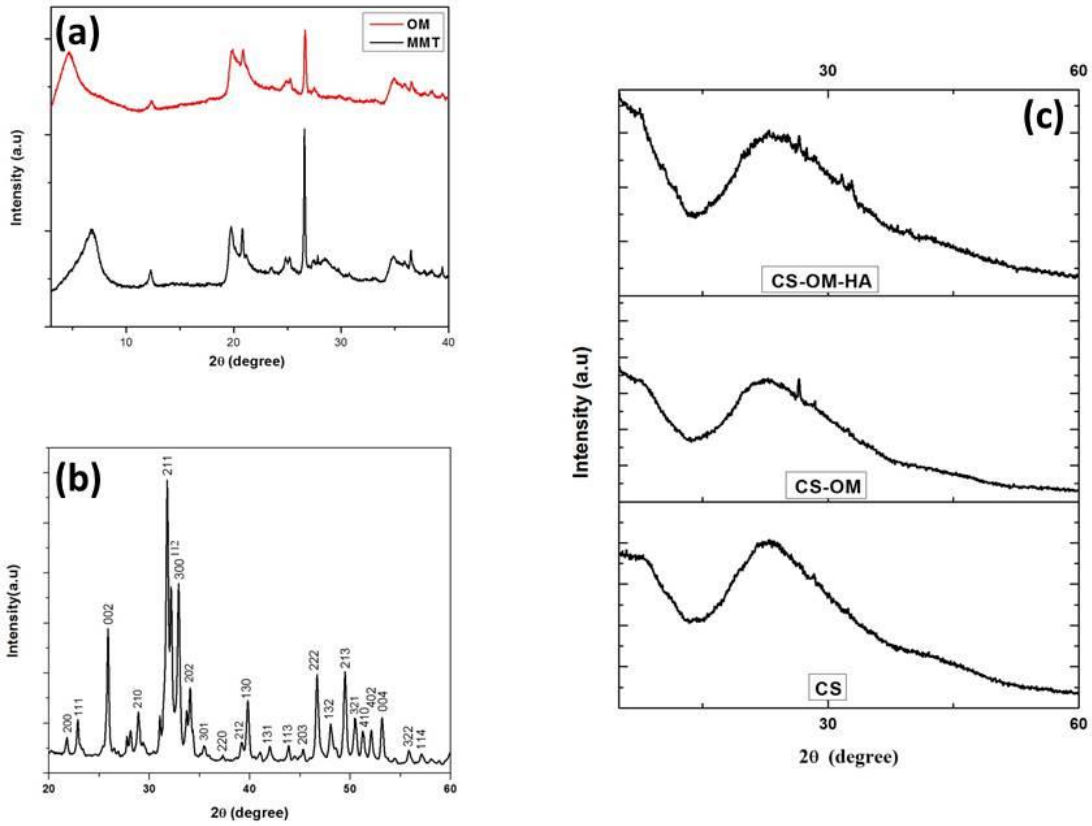


**Fig. 4 XRD patterns of (a) MMT and OM, (b) hydroxyapatite and (c) CS based composites.**

From the results, it can be concluded that presence of $PO_4^{-3}$ groups on the surface of the HA and enhanced miscibility of OM resulted into a simultaneous interaction of OM and HA with the ammonium ($NH_3^+$) ions of chitosan [20].

## 4.3 Attenuated total reflectance-fourier transform infrared (ATR-FTIR) spectroscopy

Attenuated total reflectance-fourier transform infrared spectroscopy (ATR-FTIR) provides specific information about chemical bonding and molecular structures. The ATR-FTIR spectra of the individual components (HA, OM and MMT) as well as of the CS composites (CS, CS–OM, and CS–OM-HA) are shown in Fig. 5. Band assignments for

individual components (MMT, OM and HA) as well as for the CS based composites (CS, CS–OM, and CS–OM-HA) are given in Tables I and II, respectively.

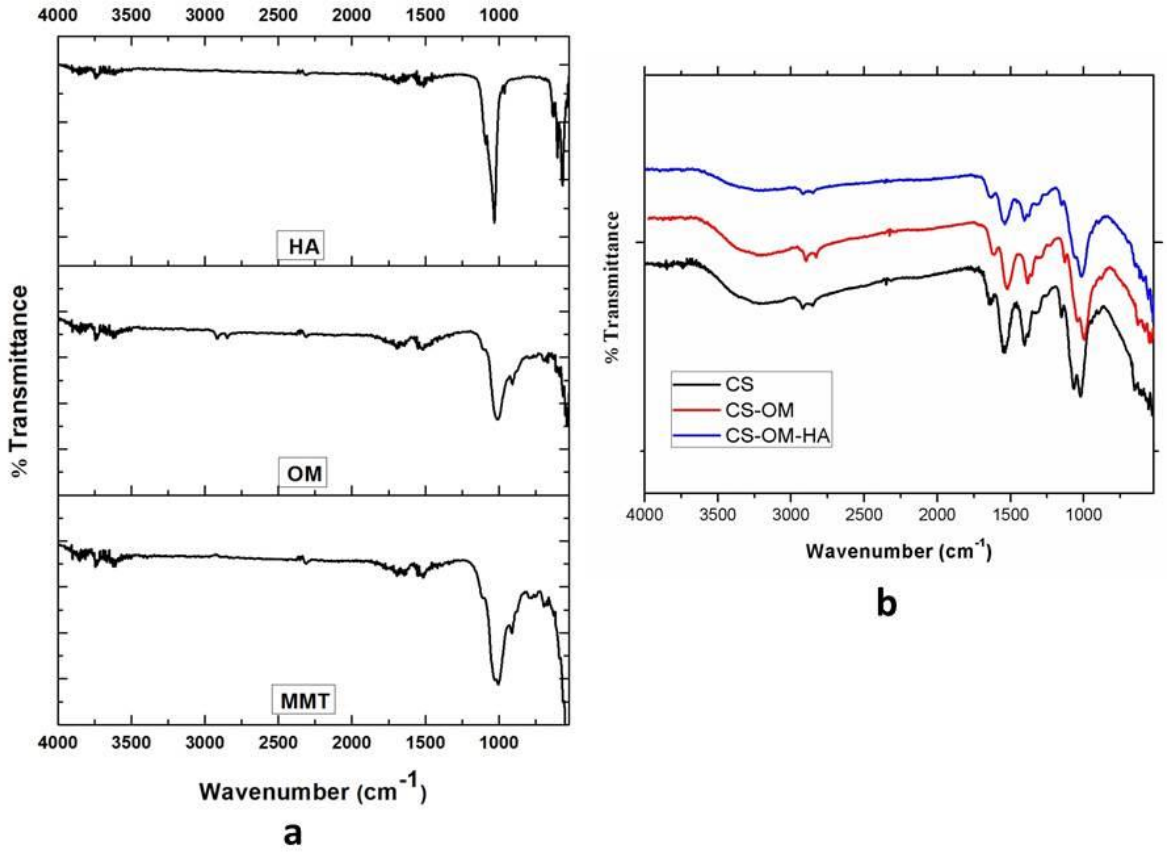


**Fig. 5 ATR-FTIR spectra of (a) HA, MMT and OM, (b) CS based composites.**

In the ATR-FTIR spectrum of MMT, the bands at 527 and 1031 $cm^{-1}$ were assigned to Si–O–Al deformation and Si–O stretching, respectively. The low intense band corresponding to OH bending of $H_2O$ was observed at 1639 $cm^{-1}$. The band related to structural OH stretching was observed at 3624 $cm^{-1}$. In case of OM, the bands related to $CH_2$ stretching modes of CTAB were observed at 2853 and 2928 $cm^{-1}$ along with the bands at 527 and 1031 $cm^{-1}$. Also, the bands associated with $OH^-$ bending of water and structural $OH^-$ stretching were shifted to 1655 $cm^{-1}$ and 3626 $cm^{-1}$, respectively [46]. The ATR-FTIR spectra of HA showed the bands related to stretching modes of $PO_4^{-3}$ were observed at 1043 and 962 $cm^{-1}$.The bands between 602–567 $cm^{-1}$ were assigned to bending vibrations of phosphate groups

present in HA.

The bands at 3570 and 630 $cm^{-1}$ were related to the stretching and liberation modes of OH, respectively. Also, low intense band of adsorbed water (stretching) was present at 1642 $cm^{-1}$ [40].

**Table I Band assignments for individual components**

| **Band Assignment** | **Wavenumber ($cm^{-1}$)** | | |
|---|---|---|---|
| | **MMT** | **OM** | **HA** |
| Structural $OH^-$ stretching | 3624 | 3626 | - |
| Stretching of $OH^-$ | - | - | 3570 |
| Asymmetric C-H stretching from CTAB | - | 2928 | - |
| Symmetric C-H stretching of CTAB | - | 2853 | - |
| OH deformation of $H_2O$ | 1639 | 1655 | - |
| Stretching from adsorbed water | - | - | 1642 |
| Asymmetric stretching of phosphate | - | - | 1043 |
| Si-O stretching from clay | 1031 | 1031 | - |
| Symmetric stretching of phosphate | - | - | 962 |
| Structural $OH^-$ | - | - | 630 |
| Bending vibrations of phosphate | - | - | 602-567 |
| Si–O–Al vibration from clay | 527 | 527 | - |

**Table II Band assignments for CS based composites**

| Band Assignment | Wavenumber ($cm^{-1}$) | | |
|---|---|---|---|
| | CS | CS-OM | CS-OM-HA |
| Structural $OH^-$ stretching from clay | - | 3626 | 3626 |
| Stretching of $OH^-$ from hydroxyapatite | - | - | 3570 |
| N-H stretching of chitosan | 3400 | 3400 | 3400 |
| C-H asymmetric stretching of chitosan | 2920 | 2915 | 2922 |
| C-H symmetric stretching of chitosan | 2851 | 2845 | 2849 |
| Amide I bands from acetamide group of chitosan | 1643 | 1640 | 1633 |
| Amide II bands from acetamide group of chitosan | 1546 | 1544 | 1538 |
| Symmetric stretching of carbonyl from $COO^-$ group | 1404 | 1403 | 1403 |
| C-H bending in amide group | 1375 | 1376 | 1374 |
| CH bending vibrations of the ring | 1324 | 1322 | 1321 |
| C–O–C in glycosidic linkage | 1153 | 1153 | 1153 |
| Si-O stretching from clay | - | 1031 | 1031 |
| Skeletal vibrations involving C–O stretching | 1067 | 1069 | 1060 |
| Skeletal vibrations involving C–O stretching | 1021 | 1020 | 1014 |
| CH deformation vibration of β-pyranose | 897 | 897 | 898 |
| O–P–O bending from hydroxyapatite | - | - | 602-567 |
| Si–O–Al vibration from clay | - | 527 | 527 |

In the pure chitosan (CS) spectrum, band corresponding to N–H stretching was observed at 3400 $cm^{-1}$ [26]. The bands at 2920 and 2845 $cm^{-1}$ correspond to the CH stretching. The broad bands at 1643 and 1546 $cm^{-1}$ were attributed the presence of amide I and amide II groups. The sharp band at 1404 $cm^{-1}$ was assigned to stretching of carbonyl from $COO^-$ group. The low intense bands at 1375 and 1321 $cm^{-1}$ were corresponded to CH bending vibrations of the ring. The characteristics peaks of C-O-C glycosidic linkage were observed in the region of 1153-1021 $cm^{-1}$. The absorption band corresponding to the CH deformation vibration of β-pyranose was observed at 897 $cm^{-1}$ [20,21]. The N-H bending region of chitosan was shifted to 1544 $cm^{-1}$ and 1538 $cm^{-1}$ in from 1546 $cm^{-1}$ in CS–OM and CS-OM-HA composites, respectively. It was also observed that the band corresponding to OH bending of $H_2O$ in OM got shifted from 1655 $cm^{-1}$ to 1659 $cm^{-1}$ and 1665 $cm^{-1}$ in CS-OM and CS-OM-HA composites, respectively. This confirms the occurrence of different interactions like hydrogen bonding and electrostatic interactions, of the chitosan with the OM and HA. However, both CS-OM and CS-OM-HA composite have shown the characteristics peaks of C-O-C glycosidic linkage and the absorption band corresponding to the CH deformation vibration of β-pyranose at 1153-1021 $cm^{-1}$ and 897 $cm^{-1}$, respectively. The bands seen near 602-567 and 3570 $cm^{-1}$ in case of CS-OM-HA composite were attributed to the O–P–O bending of phosphate group and stretching mode of OH water present in HA [20,21]. Also, the bands seen around 527, 1031, and 2928, 2853 $cm^{-1}$ in case of CS-OM and CS-OM-HA composite, correspond to the Si–O–Al deformation, Si–O stretching and CH stretching modes of OM clay, respectively. Furthermore, the structural $OH^-$ stretching of OM appeared in CS-OM and CS-OM-HA composites at 3626 $cm^{-1}$ which confirms the presence of OM in both the composites. From the ATR-FTIR spectra of the composites, it can be concluded that both OM clay and HA are successfully incorporated in the CS based composites.

## 4.4 Mechanical (tensile) properties

The composite must possess enough mechanical strength to withstand stress incurred by newly formed tissue *in vitro* till its implantation *in vivo*. The average values of the Young's modulus, tensile strength, and elongation at break of the pure CS, CS–OM and CS–OM-HA composites are reported in Table III. It was observed that there was a significant increase in tensile strength of composites over the polymer. CS-OM and CS-OM-HA composites

exhibited tensile strengths of 0.38 and 0.56 MPa, respectively. The tensile strengths have increased up to 5.5% and 55% in CS-OM and CS-OM-HA composites, respectively. Further, addition of OM and HA increased the modulus to a value of 5.02 MPa and 24.9 MPa, in CS-OM and in CS-OM-HA composites, respectively. This drastic increase in elastic modulus can attributed to the strong interfacial interactions among chitosan, OM and HA, influencing the overall mechanical properties of the CS based composites. It is well known that the interface between filler particle and polymer matrix has a significant effect on the tensile properties of the composites.

**Table III Tensile properties of CS based composites**

| Samples | Tensile strength (MPa) | Elastic modulus (MPa) | Extension at break (mm) |
|---|---|---|---|
| CS | 0.36 ± 0.057 | 4.62 ± 0.78 | 4.59 ± 0.2 |
| CS-OM | 0.38 ± 0.042 | 5.02 ± 1.85 | 5.36 ± 2.05 |
| CS-OM-HA | 0.56 ± 0.270 | 24.9 ± 3.24 | 2.56 ± 1.6 |

The elongation of the CS-OM composites have increased as compared to pure CS composite, confirming the increase in plasticity of the sample due to incorporation of OM. However, inclusion of HA induces brittleness in the CS-OM-HA composites, resulting into a reduction in elongation in CS-OM-HA as compared to pure CS. From the results, it is evident that the overall tensile property achieved in CS-OM-HA composite was the best amongst CS and CS-OM composites.

## 4.5 Water absorption study (swelling test)

The swelling of composites facilitates the infiltration of cells into the composites in a three dimensional fashion. The swelling profile of pure chitosan (CS) and its composites is shown in Fig. 6. The results have shown that incorporation of HA and OM in the polymer

matrix brought in the swelling behavior of the CS based composites. HA forms a temporary barrier preventing water permeating into the composite. HA decreases the hydrophilicity of the chitosan by binding to the hydrophilic –COOH and $–NH_2$ as well. Incorporation of OM also played a role in reduction of swelling. The sheets of OM too have formed a barrier that inhibits the interaction between polymer macromolecules and water molecules, leading into lowering of water content in both CS-OM and CS-OM-HA composites. Hence, the swelling properties of CS based composites can be tailored by using appropriate amount of inorganic phase.

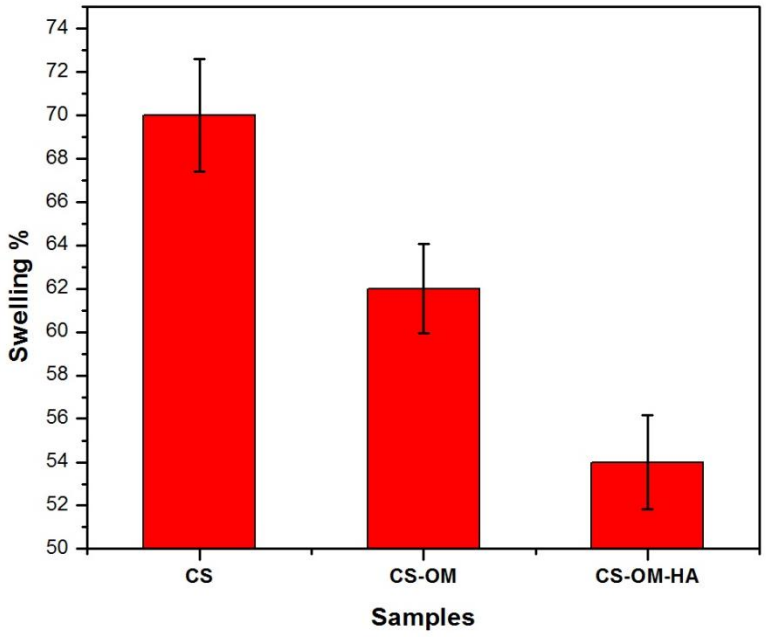


**Fig. 6 Swelling behavior of CS based composite.**

## 4.6 *In vitro* degradation

Implant materials are supposed to be degradable and the rate of degradation should match with rate of new tissue formation. The degradation profile of pure chitosan (CS), CS-OM, and CS-OM-HA composites after 28 days immersion in PBS is presented in Fig. 7. The degradation rate of pure chitosan (CS) composite was greater as compared to CS-OM, and CS-OM-HA composites and found to be decreased with the addition of OM and HA in the chitosan matrix. After 28 days of in vitro biodegradation, the mass of pure CS, CS-OM, and

CS-OM-HA composites were degraded by 32%, 23.8%, and 15.3%, respectively. Furthermore, HA dissolves slowly *in vitro* and the strong interaction between polymer macromolecule and OM clay reduce the number of hydrophilic groups in the composites. It depresses the solvent uptake thereby protects the polymer from degradation in PBS. Therefore, it can be concluded that the degradation rate can be controlled by adjusting the OM and HA contents in the polymer matrix.

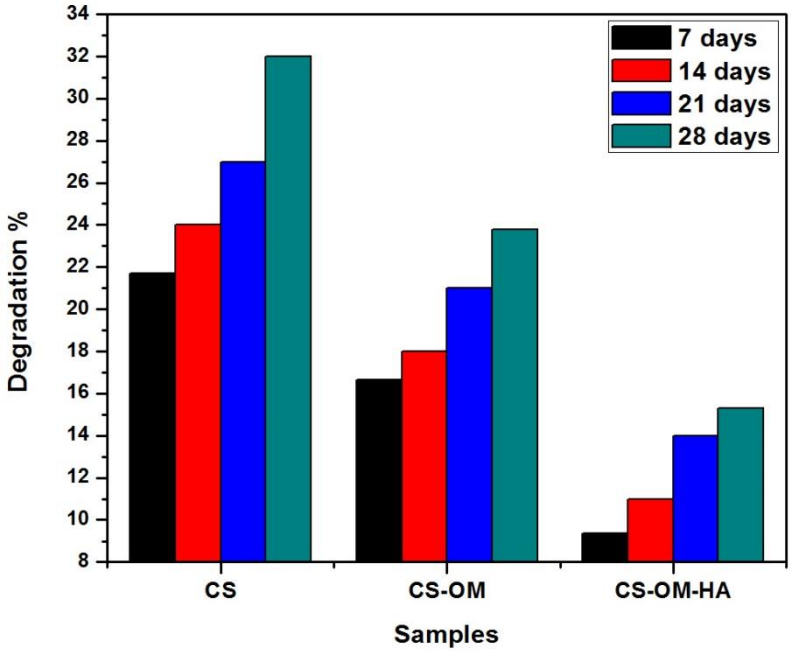


**Fig. 7 *In vitro* degradation profile of CS based composites.**

## 4.7 *In vitro* bioactivity

The CS based composites were analysed for their *in vitro* bioactivity by immersing them in SBF solution for 21 days. After 21 days, apatite formation on the surface of the composite pores was observed using scanning electron microscopy (JEOL JSM 6480LV, USA). SEM micrographs (Fig. 8) have shown apatite formation on the surface of CS based composites. The amount of apatite formation on the surfaces of the composites increased in the order of CS-OM-HA > CS-OM > CS. In this study, pure CS had no active site on its surface to trigger the apatite formation. In case of CS-OM, Si-OH (silanol) group, the chelating agents of $Ca^{+2}$ and $PO_4^{-3}$ ions present in SBF (from clay) was present on its surface,

facilitating apatite deposition [48]. HA particles acted as nucleation sites in the CS-OM-HA composites. Also, OM clay with Si-OH (silanol) group on its surface has a synergetic effect with HA to induce the apatite formation. Consequently, apatite has formed more efficiently on the CS-OM and CS-OM-HA composites than on the pure CS.

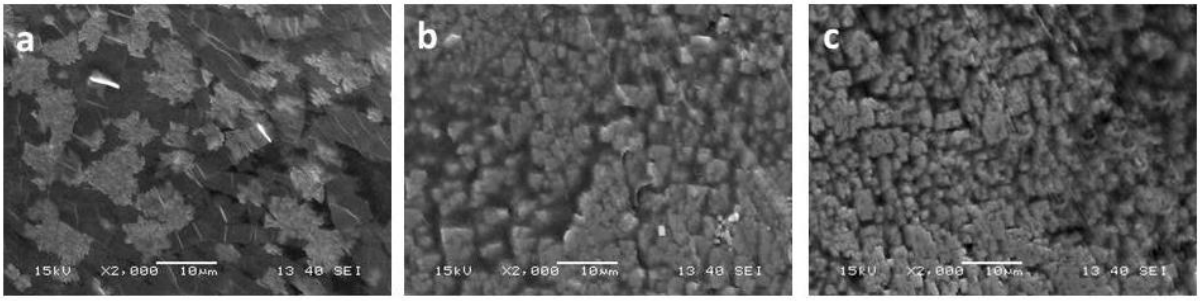


**Fig. 8 SEM micrographs showing apatite formation on (a) CS (b) CS-OM and (c) CS-OM-HA composites.**

## 4.8 Protein adsorption study

The occurrence of functional groups such as, amine ($–NH_2$), carboxyl (-COOH), and hydroxyl (-OH) on the surface of the composite greatly influences protein adsorption [49]. The amount of adsorbed BSA decreased in the sequence of CS > CS-OM > CS-OM-HA. The protein adsorption profiles of CS based composites are shown in Fig. 9. The amount of protein adsorbed reduced by 4.77% and 7.52% on CS-OM and CS-OM-HA composites, as compared to pure CS. In this study, the presence of aforementioned hydrophilic groups in pure CS resulted in highest protein adsorption among CS-OM and CS-OM-HA composites. The interaction with the hydrophilic groups (-COOH, -OH, $–NH_2$) became more prominent in the presence of PBS as a solubilising medium. Montmorillonite had hydroxyl (-OH) groups on its surface, but CTAB modification incorporated cations in place of anionic hydroxyl (-OH) groups [15]. Consequently, active sites (hydrogen bond forming sites) for BSA attachment were no longer available on the surface of organically modified montmorillonite, led to the formation of a complex with CS that had less affinity towards BSA. Basu *et al*. have reported that hydroxyapatite interacts electrostatically with BSA via electrostatic interaction between the $Ca^{+2}$ cations and $PO_4^{-3}$ anions of HA with the $COO^-$ anion and $NH_3^+$ cations of the BSA protein, respectively [50].

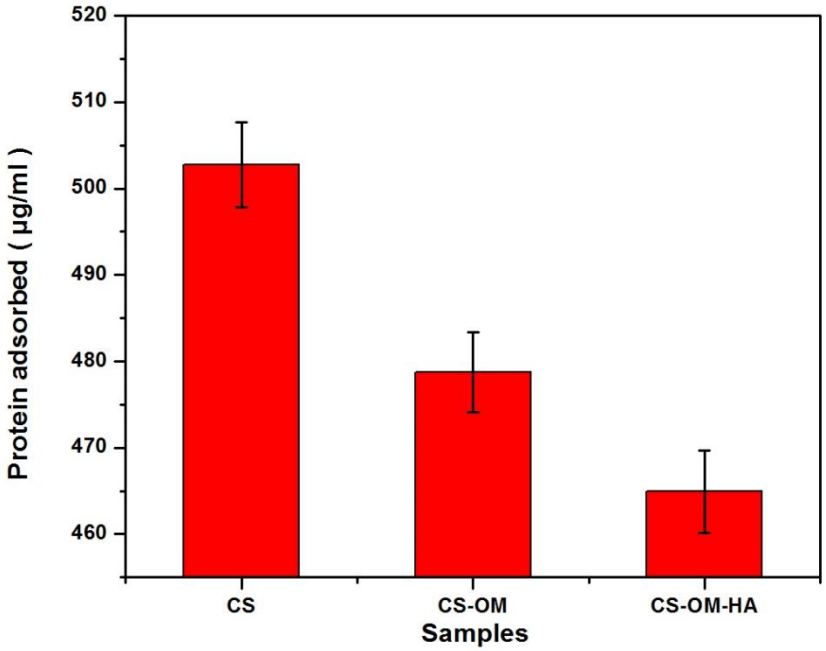


**Fig. 9 Protein adsorption profile of CS based composite.**

However, in case of CS-OM-HA composite these active sites for BSA interaction were already taken up by $COO^-$ and $NH_3^+$ of chitosan. Hence, no active site was present on the surface of HA to interact with BSA. From the results, it can be concluded that the addition of HA and OM would suppress of non-specific protein adsorption, which could reduce the fibrosis tissue thickness and macrophages adhesion *in vivo.*

## 4.9 Cell viability assay

Osteoblast cells' response on CS based composites was investigated by MTT assay. The MTT assay results demonstrated (Fig.10) a significant increase in cell viability of all composites as compared to previous study [21]. Katti *et al.* have reported 40% and 28% cell viability with CS-MMT and CS-HA-MMT scaffolds, respectively [21]. But incorporation of OM into the polymer matrix in place of MMT has induced a drastic increase of cell viability of CS-OM (68.5%) and CS-OM-HA (54.5%) composites, respectively. Sirousazar *et al.* have already reported cytocompatibility of OM containing PVA/clay nanocomposite hydrogels towards K562 (erythroleukemia) cell line [51]. From the results, it can be concluded that the CS based composites were non-cytotoxic to MG 63 cell line.

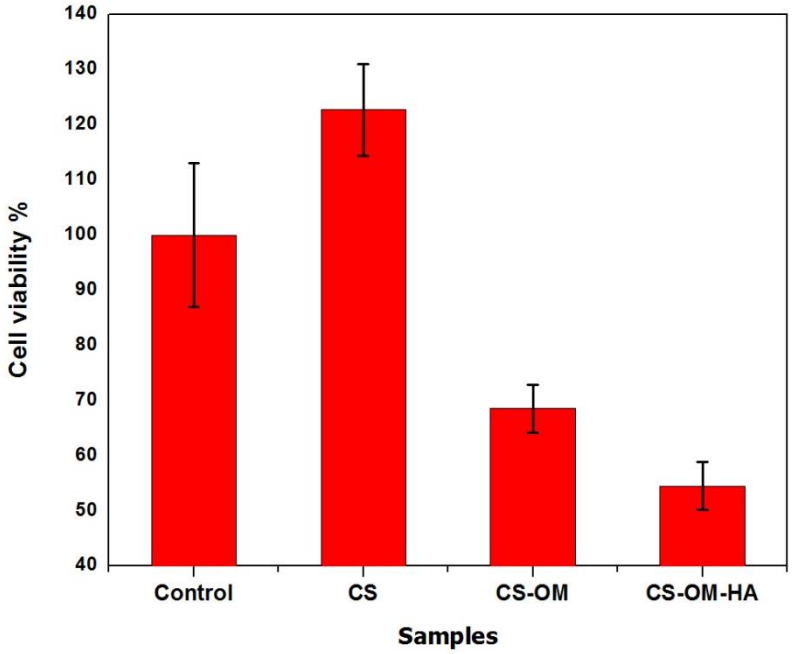


**Fig. 10 Cell viability results of CS based composite.**

# CHAPTER 5

# CONCLUSION

## 5. CONCLUSION

A novel CS-OM-HA was synthesized by combining microwave irradiation and gas foaming method with pores in the sizes of micro range. A reduction in pore size was observed in this composite as compared to pure CS and CS-OM composites. The XRD results indicated the formation of an exfoliated structure. ATR-FTIR study demonstrated the evidence of strong molecular interaction among the three different constituents of the composite, which can be clearly observed from the shift in the band position of chitosan in the presence of OM and HA. Improved mechanical property and bioactivity was observed with the incorporation of OM and HA. The swelling, degradation and protein adsorption of CS-OM-HA composites were lowered in comparison to the pure CS and CS-OM composites. Cytotoxicity studies showed the prepared composites were non-toxic when tested with MG 63 cell line. From the results, it can be concluded that the novel CS-OM-HA composites can be a potential biomaterial for non-load bearing orthopedic applications.

## REFERENCES


1. M.M. Stevens, Biomaterials for bone tissue engineering: A Review, Mater. today 11 (2008) 18-25.
2. R. Jayakumar, D. Menon, K. Manzoor, S.V. Nair, H. Tamura, Biomedical applications of chitin and chitosan based nanomaterials – A short review, Carbohydr. Polym. 82 (2010) 227–232.
3. J.K.F. Suh, H.W.T. Matthew, Application of chitosan-based polysaccharide biomaterials in cartilage tissue engineering: A Review, Biomaterials 21 (2000) 2589–2598.
4. J.S. Mao, L.G. Zhao, Y.J. Yin, K.D. Yao, Structure and properties of bilayer chitosan–gelatin, Biomaterials 24 (2003) 1067–1074.
5. F.H. Lin, C.H. Yao, J.S. Sun, H.C. Lin, C.W. Huang, Biological effects and cytotoxicity of the composite composed of tricalcium phosphate and glutaraldehyde cross-linked gelatin, Biomaterials 19 (1998) 905-917.
6. G. Tripathi, B. Basu, A porous hydroxyapatite scaffold for bone tissue engineering: physico-mechanical and biological evaluations, Ceram. Int. 38 (2012) 341–349.
7. C. Xianmia, L. Yubao, Z. Yi, Z. Li, L. Jidong, W. Huanan, Properties and in vitro biological evaluation of nano hydroxyapatite/chitosan membranes for bone guided regeneration. Mater. Sci. Eng. C 29 (2009) 29–35.
8. L. Kong, Y. Gao, W. Cao, Y. Gong, N. Zhao, X. Zhang, Preparation and characterization nanohydroxyapatite/chitosan composite scaffold, J. Biomed. Mater. Res. 5 (2005) 275–82.
9. L. Kong, Y. Gao, W. Cao, Y. Gong, N. Zhao and X. Zhang, A study on the bioactivity of chitosan/nano-hydroxyapatite composite scaffolds for bone tissue engineering, Eur. Polym. J. 42 (2006) 3171–3179.
10. H. Qiaoling, L. Baoqiang, W. Mang, S. Jiacong, Preparation and characterization of biodegradable chitosan/hydroxyapatite nanocomposite rods via in situ hybridization: a potential material as internal fixation of bone fracture, Biomaterials 25 (2004) 779–785.

11. M. Ito, Y. Hidaka, M. Nakajima, H. Yagasaki, A. H. Kafrawy, Effect of hydroxyapatite content on physical properties and connective tissue reactions to a chitosan–hydroxyapatite composite membrane, J. Biomed. Mater. Res. 45 (1999) 204–208.
12. A.K. Mishra, S. Allauddin, R. Narayan, T.M. Aminabhavi, K.V.S.N. Raju, Characterization of surface-modified montmorillonite nanocomposites, Ceram. Int. 38 (2012) 929–934.
13. J.P. Zheng, C. Z. Wang, X.X. Wang, H.Y. Wang, H. Zhuang, K.D. Yao, Preparation of biomimetic three-dimensional gelatin/montmorillonite–chitosan scaffold for tissue engineering, React. Funct. Polym. 67 (2007) 780–788.
14. A. H. Ambre, K. S. Katti, D. R. Katti. Nanoclay Based Composite scaffolds for Bone Tissue Engineering Applications. J. Nanotech. Eng. Med.1 (2010) 0310131-9.
15. M. Kokabi, M. Sirousazar, Z. M. Hassan, PVA–clay nanocomposite hydrogels for wound dressing, Eur. Polym. J. 43 (2007) 773–781.
16. A. Pandey, G.C. Pandey, P. Aswath, Synthesis of polylactic acid–polyglycolic acid blends using microwave radiation, J. Mech. Behav. Biomed. Mater. 1 (2008) 227-233.
17. I.G. Beşkardeş, T.T. Demirtaş, M.D. Durukan, M. Gümüşderelioğlu, Microwave-assisted fabrication of chitosan–hydroxyapatite superporous hydrogel composites as bone scaffolds. J. Tissue. Eng. Regen. Med. 2012 Dec 14 DOI: 10.1002/term.1677
18. S.F. Wang , L. Shen , Y.J. Tong , L. Chen , I.Y. Phang , P.Q. Lim , T.X. Liu, Biopolymer chitosan/montmorillonite nanocomposites: Preparation and characterization, Polym. Degrad. Stabil. 90 (2005) 123-131.
19. H. Zhuang, J.P. Zheng, H. Gao, K.D. Yao, *In vitro* biodegradation and biocompatibility of gelatin/montmorillonite-chitosan intercalated nanocomposite. J. Mater. Sci: Mater. Med. 18 (2007) 951–957.
20. A. Olad, F. F. Azhar, The synergetic effect of bioactive ceramic and nanoclay on the properties of chitosan–gelatin/nanohydroxyapatite–montmorillonite scaffold for bone tissue engineering. Ceram. Int. 40 (2014) 10061–10072.
21. K.S. Katti, D.R. Katti, R. Dash, Synthesis and characterization of a novel chitosan/montmorillonite/hydroxyapatite nanocomposite for bone tissue engineering, Biomed. Mater. 3 (2008) 034122-33.

22. W.W. Thein-Han, R.D.K. Misra. Biomimetic chitosan nanohydroxyapatite composite scaffolds for bone tissue engineering, Acta. Biomater. 5 (2009) 1182–1197.
23. M. Swetha, K. Sahithi, A. Moorthi, N. Srinivasan, K. Ramasamy, N. Selvamurugan. Biocomposites containing natural polymers and hydroxyapatite for bone tissue engineering, Int. J. Biol. Macromol. 47 (2010) 1–4.
24. S. Ramakrishna, J. Mayer, E. Wintermantel, K.W. Leong, Biomedical applications of polymer-composite materials- A review, Compos. Sci. Technol. 61 (2001) 1189–1224.
25. K. Madhumathi, K.T. Shalumon, V.V.D. Rani, H. Tamura, T. Furuike, N. Selvamurugan, S.V. Nair, R. Jayakumar, Wet chemical synthesis of chitosan hydrogel–hydroxyapatite composite membranes for tissue engineering applications, Int. J. Biol. Macromol. 45 (2009) 12–15.
26. X.J. Tang, L. Gui, X.Y. Lu, Hard tissue compatibility of natural hydroxyapatite/chitosan composite, Biomed. Mater. 3 (2008) 44115-23.
27. M. Jayabalan, K.T. Shalumon, M.K. Mitha, K. Ganesan, M. Epple, Effect of hydroxyapatite on the biodegradation and biomechanical stability of polyester nanocomposites for orthopaedic applications, Acta. Biomater. 6 (2010) 763-775.
28. Y. Zhang, J.R. Venugopal, A. El-turki, S. Ramakrishna, B. Su, C.T. Lim, Electrospun biomimetic nanocomposite nanofibers of hydroxyapatite/chitosan for bone tissue engineering, Biomaterials 29 (2008) 4314–4322.
29. H. Kashiwazaki, Y. Kishiya, A. Matsuda, K. Yamaguchi, T. Iizuka, J. Tanaka, N. Inoue, Fabrication of porous chitosan/hydroxyapatite nanocomposites: Their mechanical and biological properties. Biomed. Mater. Eng. 19 (2009) 33–40.
30. K. Shen, Q. Hu, L. Chen, J. Shen, Preparation of chitosan biocomponent nanofibers filled with hydroxyapatite nanoparticles via electrospinning, J. Appl. Polym. Sc. 115 (2010) 2683–2690.
31. P. Kithva, L. Grondahl, D. Martin, M. Trau, Biomimetic synthesis and tensile properties of nanostructured high volume fraction hydroxyapatite and chitosan biocomposite films, J. Mater. Chem. 20 (2010) 381–389.
32. F. Zhao, Y. Yin, W.W. Lu, J.C. Leong, W. Zhang, J. Zhang, K. Yao, Preparation and histological evaluation of biomimetic three-dimensional hydroxyapatite/chitosan-gelatin network composite, Biomaterials 23 (2002) 3227–3234.

33. F. Zhao, W.L. Grayson, T. Ma, B. Bunnell, W.W. Lu, Effects of hydroxyapatite in 3-D chitosan–gelatin polymer network on human mesenchymal stem cell construct development, Biomaterials 27 (2006) 1859–1867.
34. J. Liuyun, L. Yubao, X. Chengdong, Preparation and biological properties of a novel composite scaffold of nano-hydroxyapatite/chitosan/carboxymethyl cellulose for bone tissue engineering, J. Biomed. Sci. 16 (2009) 65–74.
35. A. Okada, M. Kawasumi, A. Usuki, Y. Kojima, T. Kurauchi, O. Kamigaito, "Synthesis and properties of nylon-6/clay hybrids" Polymer Based Molecular Composites, MRS Symposium Proceedings, D. W. Schaeferand J. E. Mark, eds. 171 (1990) 45–50.
36. D. Sikdar, D.R. Katti, K.S. Katti, B. Mohanty, Influence of Backbone Chain Length and Functional Groups of Organic Modifiers on Crystallinity and Nanomechanical Properties of Intercalated Clay-Polycaprolactam Nanocomposites, Int. J. Nanotechnol. 6 (2009) 468–492.
37. H. Ge, S. Huang, Microwave preparation and adsorption properties of EDTA modified cross-linked chitosan, J. Appl. Polym. Sci. 115 (2010) 514–519.
38. S.H. Lee, W.G. Lee, B.G. Chung, J. H. Park, A. Khademhosseini, Rapid formation of acrylated microstructures by microwave-induced thermal crosslinking, Macromol. Rapid. Commun. 30 (2009) 1382–1386.
39. S. Shi, L. Liu, Microwave-assisted preparation of temperature sensitive poly (N-isopropylacrylamide) hydrogels in poly-(ethylene oxide)-600, J. Appl. Polym. Sci. 102 (2006) 4177–4184.
40. X. Guo, H. Yan, S. Zhao, L. Zhang, Y. Li, X. Liang, Effect of calcining temperature on particle size of hydroxyapatite synthesized by solid-state reaction at room temperature, Adv. Powder Technol. 24 (2013) 1034–1038.
41. T. Kokubo, H. Takadama, How Useful is SBF in Predicting *In Vivo* Bone Bioactivity?, Biomaterials 27 (2006) 2907-2915.
42. Standard test method for tensile properties of polymer matrix composite materials, D3039M-00 (2002), ASTM International, West Conshohocken, PA 19428-2959
43. S.Yang, K.F. Leong, Z. Du, C.K. Chua, The design of scaffolds for use in tissue engineering. Part I. traditional factors, Tissue Eng. 7(6) (2001) 679–89.

44. N. Rameshbabu, T. S. Sampath Kumar, K. Prasad Rao, Synthesis of nanocrystalline fluorinated hydroxyapatite by microwave processing and its *in vitro* dissolution study, Bull. Mater. Sci. 29 (6) (2006) 611–615.
45. M.S. Pendekal, P.K. Tegginamat, Hybrid drug delivery system for oropharyngeal, cervical and colorectal cancer–in vitro and in vivo evaluation, Saudi. Pharm.J. 21 (2013) 177–186.
46. M. Koosha, H. Mirzadeh, M.A. Shokrgozar, M. Farokhi, Nanoclay-reinforced electrospun chitosan/PVA nanocomposite nanofibers for biomedical application, RSC Adv. 5 (2015) 10479-87.
47. M. Alshabanat, A. Al-Arrash, W. Mekhamer, Polystyrene/Montmorillonite Nanocomposites: study of the morphology and effects of sonication time on thermal stability. J. Nanomat. (2013) 650725, 1-12.
48. I. Grigoriadou, N. Nianias, A. Hoppe, Z. Terzopoulou , D. Bikiaris , J. Will, J. Hum, J.A. Roether, R. Detsch, A.R. Boccaccini, Evaluation of silica-nanotubes and strontium hydroxyapatite nanorods as appropriate nanoadditives for poly-(butylene succinate) biodegradable polyester for biomedical applications, Compos Part B-Eng 60 (2014) 49–59.
49. D. Depan, R.D.K. Misra, The interplay between nanostructured carbon-grafted chitosan scaffolds and protein adsorption on the cellular response of osteoblasts: Structure–function property relationship, Acta. Biomater. 9 (2013) 6084-6094.
50. B. Basu, S.K. Swain, D. Sarkar, Cryogenically cured hydroxyapatite–gelatin nanobiocomposite for bovine serum albumin protein adsorption and release, RSC Adv. 3 (2013) 14622-33.
51. M. Sirousazar, M. Kokabi, Z. M. Hassan, *In Vivo* and Cytotoxic Assays of a Poly(vinyl alcohol)/Clay Nanocomposite Hydrogel Wound Dressing, J. Biomater. Sci. Polym. Ed. 22 (2011) 1023–1033.